

# **Inactivation of water pathogens with solar photo-activated persulfate oxidation**

L. C. Ferreira<sup>a</sup>, M. Castro-Alfárez<sup>b</sup>, S. Nahim-Granados<sup>b</sup>, M.I. Polo-López<sup>b</sup>, M. S.

Lucas<sup>a,c\*</sup>, G. Li Puma<sup>c</sup>, P. Fernández-Ibáñez<sup>b,d</sup>

<sup>a</sup> Centro de Química de Vila Real, Universidade de Trás-os-Montes e Alto Douro,  
5000-801 Vila Real, Portugal

<sup>b</sup> Plataforma Solar de Almería – CIEMAT, P.O. Box 22, 04200 Tabernas, Almería,  
Spain

<sup>c</sup> Environmental Nanocatalysis & Photoreaction Engineering, Department of Chemical  
Engineering, Loughborough University, Loughborough, LE11 3TU, United Kingdom

<sup>d</sup> Nanotechnology and Integrated BioEngineering Centre, School of Engineering,  
University of Ulster, Newtownabbey, Northern Ireland BT37 0QB, United Kingdom

\*Corresponding authors:

Marco S. Lucas; [mlucas@utad.pt](mailto:mlucas@utad.pt)

Pilar Fernández-Ibáñez; [p.fernandez@ulster.ac.uk](mailto:p.fernandez@ulster.ac.uk)

## ABSTRACT

This contribution investigates the effect of solar activated persulfate and solar mild thermal heating for water disinfection (PS/solar). The basic effects of solar ultraviolet (UV) and thermal increase were separately studied for the inactivation of *E. coli* and *E. faecalis*. The process was studied in isotonic water (IW) and synthetic urban wastewater (SUWW) at bench and pilot scale (60 L-solar compound parabolic collector reactor). The thermal inactivation at 40 °C and 0.5mM-PS shows a 3 log reduction value (LRV) for *E. coli* without lag phase and 5-LRV for *E. faecalis* with a lag phase of 1h, in 4 h of exposure. At 50 °C the mere effect of temperature, overlaps the thermal activation of PS, being markedly fast. Effective accelerated disinfection effect by PS/solar (UVA and thermal) was observed. 6-LRV in *E. coli* and *E. faecalis* was determined for solar exposure periods of 20 min (solar dose), using 0.5 and 0.7 mM of PS in isotonic water, respectively. Longer solar exposure times were required to attain similar LRV in synthetic urban wastewater, in the presence of 25 mg/L of organic matter, i.e. 80 and 100 min (solar dose) for *E. coli* and *E. faecalis*, respectively. These results were confirmed at pilot scale, where 60 L of isotonic water were treated with 0.5 mM of PS in 50 min (solar dose). The PS/solar uses low cost chemical reagents (0.5 mM-PS) and a free source of energy (solar) to treat wastewater and achieve the high removal (6-LRV) of two model faecal indicators of water contamination, which opens a clear alternative to treat polluted water with organic matter and pathogens with implications in water-energy reclamation field.

**Keywords:** Compound Parabolic Collector; Persulfate; Solar UVA; Solar thermal; Sulfate radicals; Water disinfection.

## 1. INTRODUCTION

Today the world is suffering one of the worst crises in relation to fresh water sources, in terms of scarcity and quality. Usually water pollutants are organic contaminants, nutrients and waterborne pathogens, which have to be removed using conventional or new technologies to reduce health and environmental risks. The waterborne diseases triggered by pathogenic microorganisms pose a high threaten to human health and the environment. Therefore, water disinfection is a critical step to improve the quality of our water resources for a number of applications, i.e. irrigation, domestic and even, more importantly, for drinking. In the case of low income countries, the lack of clean and safe (free of pathogens) water is the major cause of the spread of waterborne diseases and of high incidence of water related mortality and morbidity [1,2].

Microbiological assessment of water quality is usually carried out through the measurement of indicator microorganisms' concentration. *Escherichia coli* is the most commonly indicator of faecal contamination studied in wastewater disinfection. *E. coli* is a Gram-negative coliform bacterium frequently present in untreated surface waters and in faecal contaminated water. Moreover, *E. coli* is recognised as the third most important pathogen responsible for childhood diarrhoea [3]. It is one of the most sensitive pathogens to disinfection techniques. Another frequently recognised indicator of faecal contamination is the Gram-positive bacterium *Enterococcus faecalis*, which is the most predominant intestinal enterococci [4]. This bacterium is highly present in the excreta of warm blooded animals and in polluted wastewater, while it is not present in clean waters or any other sources that have not been in contact with human or animal life. Therefore, the WHO recommended the monitoring of *E. faecalis* as an indicator of faecal pollution in contaminated water. *E. faecalis* is usually more resistant than *E. coli* to most of the disinfection techniques or processes [5,6].

A number of conventional disinfection processes have been traditionally used such as chlorination, UV treatment (meaning UVC lamps) and ozone. These processes offer a strong capacity for the inactivation and killing of a wide range of pathogens in water, but they may also generate carcinogenic disinfection by products such as trihalomethanes and haloacetic acids by chlorination of water with a given content of natural organic matter. UV and ozone systems are very effective for a number of pathogens but, unlike chlorine, they do not have a residual disinfection capacity after treatment. They usually require high capital, operational and maintenance costs, which are associated to the complexity of the technology. Proposing alternative water disinfection solutions that overcome these drawbacks have been recently arisen via novel disinfection photo-chemical processes. Some of these processes use photons from lamps or the sun for the photoexcitation of specific molecules and catalysts to the generation of a number of oxidising species (hydroxyl radicals, singlet oxygen and hydrogen peroxide) that will compromise the viability of water microorganisms mostly via oxidative routes. Most of these studies belong to the so-called advanced oxidation processes (AOPs), including  $\text{H}_2\text{O}_2/\text{UVC}$ , heterogeneous photocatalysis, photo-Fenton and  $\text{H}_2\text{O}_2/\text{O}_3$  [7-12]. Interestingly, some of these processes can be promoted by harvested solar radiation, with the corresponding advantages of cost and energy saving by using lamps. These are solar photo-induced processes [13], like solar water disinfection [14], solar photocatalysis or solar photo-Fenton [15].

Sulfate radical-based advanced oxidation processes (SR-AOPs) have been described as an efficient treatment to inactivate pathogenic microorganisms in water [16-19]. Persulfate ( $\text{S}_2\text{O}_8^{2-}$ , PS), is one via of sulfate radicals ( $\text{SO}_4^{\bullet-}$ ) generation, characterized by being stable at ambient temperature, having high solubility and non-toxicity [20-22]. The redox potential of  $\text{SO}_4^{\bullet-}$  is between 2.5 and 3.1 V (pH dependent), being near to the

hydroxyl radical potential ( $E^0 = 1.8-2.7$  V), which suggests a good behaviour in water treatment [22-25].

The activation of PS with heat or UV radiation ends in the homolytic cleavage of the peroxide bond and the formation of  $SO_4^{\bullet-}$  (equation 1) [26]. As the molecular structure of PS is symmetric regarding the peroxide bond, then the heat/UV activation results in two sulfate radicals.



As this process is temperature dependant, a decrease in the production of sulfate radicals is noticed below 20 °C when applied to *in situ* chemical oxidation [27]. Thermolytic generation of sulfate radicals was demonstrated at 30 and 37 °C for the degradation of microcystin-LR [26]. Huang and Huang (2009) reported the mineralization of bisphenol A by heat activated PS oxidation, showing that increasing the temperature from 25 to 50 °C, higher degradation rates were obtained [28]. Potakis et al. (2017) demonstrated that the activation by temperature appears to be the single most important parameter, i.e. a temperature increase from 40 to 70 °C results in an 80-fold rate increase in the oxidation of bisphenol A [29].

The UV activation of persulfate has been extensively explored with UVA-vis and UVC lamps. In fact, the generation of sulfate radicals increases by decreasing the wavelength. This can be explained by the high extinction coefficients of PS activated by low UV wavelengths ( $\lambda_{PS} = 248$  nm,  $\epsilon_{PS} = 27.5$  M<sup>-1</sup> cm<sup>-1</sup>;  $\lambda_{PS} = 308$  nm,  $\epsilon_{PS} = 1.18$  M<sup>-1</sup> cm<sup>-1</sup>;  $\lambda_{PS} = 351$  nm,  $\epsilon_{PS} = 0.25$  M<sup>-1</sup> cm<sup>-1</sup>) [30]. As for other photo-activated processes, the wavelength dependence of absorptivity is reported. Sulfate radicals are known to yield low absorption in the UV-vis spectra ( $\lambda_{SO_4} = 450$  nm,  $\epsilon_{SO_4} = 1100$  M<sup>-1</sup> cm<sup>-1</sup>;  $\lambda_{SO_5} =$

260 nm,  $\epsilon_{SO_5} = 1030 \text{ M}^{-1} \text{ cm}^{-1}$ ;  $\lambda_{SO_3} = 250 \text{ nm}$ ,  $\epsilon_{SO_3} = 1380 \text{ M}^{-1} \text{ cm}^{-1}$ ) and brief half-life time ( $t_{1/2}=30$  to  $40 \mu\text{s}$ ). The highest absorption rate occurs in the UVC range, between 200 and 254 nm, yet PS can be activated between 193 and 351 nm, being possible to attain even higher absorption values when the oxidant concentrations are above mM levels [26,31]. Despite the low absorbance values, radiation is able to activate PS due to the high quantum yield at low wavelength values. Hermann and co-authors (2007) confirmed this statement through the calculation quantum yields formation of  $\text{SO}_4^{\cdot-}$  by the photolysis fission of PS ( $\lambda = 248$ ,  $\Phi = 1.4 \pm 0.3$ ;  $\lambda = 308$ ,  $\Phi = 1.1 \pm 0.2$ ;  $\lambda = 351$ ,  $\Phi = 0.5 \pm 0.1$ ) [32].

SR-AOPs efficiency in disinfection has been reported by several authors with different activation pathways [6,17,25,33,34]. Bianco and collaborators (2017) described PS (0.5 mM) activation with  $\text{Fe}^{3+}$ /EDDS (S,S- Ethylenediamine-N,N'-disuccinic acid trisodium salt solution, 0.1 mM) and visible light, in which *Enterococcus faecalis* is eliminated after 180 minutes [6]. A slightly different approach using a catalyst and a white LED lamp for PS activation is the ilmenite/PS/vis system ( $1 \text{ gL}^{-1}/0.5 \text{ mM}/3 \text{ mWcm}^{-2}$ ). In this case, the faecal pathogen, *E. coli*, was completely removed in 20 minutes (6-LRV) [34]. Heat, solar UV (Xenon lamp with infrared and UV-C,  $900 \text{ Wm}^{-2}$ ) and  $\text{Fe}^{2+}$  (1 mg/L) in PS activation were evaluated using MS2 bacteriophage and *E. coli* K12 as targets. In *E. coli* K12, the solar UV-C activation was the best activator *de per se* (6-log decay in 180 minutes), while the combination of heat/solar UV-C/ $\text{Fe}^{2+}$  could attained the higher synergistic factor (2.21) with 6-LRV in 60 minutes, using 0.09 mM of PS and  $T= 40^\circ \text{ C}$ . Heat activation (30, 40 and  $50^\circ \text{ C}$ ) by itself revealed that only the higher temperature was able to properly inactivate the microorganism [25].

This work presents for the first time, the effect of natural solar radiation and solar mild thermal heating at bench and at pilot scale for the disinfection of natural water and

synthetic urban wastewater (SUWW), as can be confirmed by Xiao and co-authors (2019) [35]. This work investigates both, i) the optical activation of PS by solar photons (PS/solar UVA), and ii) the thermal activation of PS via solar heating (PS/solar thermal). The basic effects of solar UV wavelengths and thermal increase have been separately studied for the inactivation of *E. coli* and *E. faecalis*. The process has been studied in isotonic water (IW) and synthetic urban wastewater (SUWW) at both laboratory and pilot scale (60 L-solar CPC reactor) under natural solar radiation.

## 2. MATERIAL AND METHODS

### 2.1 Enumeration/quantification of bacteria

*E. coli* (CECT 4624) and *E. faecalis* (CECT 5143) strains were obtained from the Spanish Type Culture Collection (CECT). Fresh liquid cultures were prepared in Luria-Bertani nutrient medium (LB Broth) and incubated at 37 °C with rotary shaking for 20 h ( $10^9$  CFU/mL). The bacterial suspensions were centrifuged at 2500 rpm for 10 minutes and the pellets were re-suspended in a phosphate-buffered saline (PBS) solution. The initial bacterial concentrations in the reactors were  $10^6$  CFU mL<sup>-1</sup>. Samples were evaluated by the standard plate counting method using Slanetz Bartley agar for *E. faecalis* and Endo agar for *E. coli*. Serial 10-fold dilutions in PBS were made dropping 20 µL (3 replicates) of each diluted sample over the corresponding agar medium. The detection limit was 17 CFU/mL (1 CFU per 60 µL). The plates were incubated at 37 °C during 24 h for *E. coli* and 42 h for *E. faecalis*, prior to viable colonies count and enumeration calculations with statistical analysis.

## **2.2 PS determination**

Sodium persulfate ( $\text{Na}_2\text{S}_2\text{O}_8$ , Panreac) was measured according to an adapted spectrometric procedure described by Liang et al. (2008) using a T60 spectrometer, PG instruments [36]. In summary, 0.5 mL of sodium hydrogen carbonate ( $\text{NaHCO}_3$ , Sigma) was added to 1 mL of sample, 3.5 mL of potassium iodine (KI, Panreac) was also added at the same time; 15 minutes later, the optical absorption of the solution was measured at 352 nm. The concentrations of PS used in this work were 0.01, 0.05, 0.1, 0.2, 0.5, 0.7 and 1 mM. This spectrophotometric method permits to differentiate between persulfate anion and sulfate radicals simultaneously. In order to evaluate the accuracy of this method, and considering that the ferrous iron is able to activate PS [25], we made an experiment of adding persulfate and ferrous sulfate to water and then expose it to solar radiation during 1 hour. Simultaneously, the same experiment was made without ferrous sulfate (Figure S1). The concentrations were used in a proportion 1:5 as reported elsewhere [25]: 0.1 mM of ferrous sulfate and 0.5 mM-PS. An additional dosage of 0.2 mM of ferrous sulfate was also tested. The results clearly showed the activation of PS by ferrous sulfate when the values of persulfate anion are lowering during the experiment. In the case of UVA PS activation, the generation of radicals cannot be confirmed, once there was no difference in the values measured.

## **2.3 Water matrices**

The disinfection experiments were performed in two water matrices: isotonic water (IW) made of distilled water with sodium chloride (0.9% w/v) and synthetic urban wastewater (SUWW) which was prepared as described elsewhere [37]. This model wastewater was used to investigate the process under more realistic conditions.



## ***2.4 Disinfection experiments***

The experiments were carried out at Plataforma Solar de Almería, Southeast of Spain, located at 37°84N and 2°34W. Solar tests were performed in sunny days, in consecutive days during summer in 2 months, between 10:30-15:30, local time.

The reagents and the pathogens suspension were diluted into the reactor covered to obtain  $10^6$  CFU/mL prior to solar exposure according to the following procedure. An appropriate dose of persulfate, when used, was added to the water matrix with the stirring on, followed by the bacterial suspension which was maintained under continuous stirring for 5 min. After the collection of the first sample, the experiment started by exposing the reactor to solar light. The water temperature was monitored directly in the reactors using a thermometer (Checktemp, Hanna instruments).

Samples collected from the reactor at regular intervals during the 5 h were immediately diluted and analysed according to the aforementioned bacterial quantification methods. Each operational condition was tested in triplicate in consecutive days for similar solar irradiance. Results obtained from the replicates had high reproducibility (95 % confidence level), and bacterial inactivation in each graph is represented as the average of the replicated with their corresponding standard deviation as error bar.

### ***2.4.1 PS-thermal experiments (dark)***

A dark test of bacteria with PS was done in order to determine the mere effect of PS over bacteria viability at room temperature (25 °C). Moreover, the thermal effect of PS was studied using a cool-hotter dry and dark incubator with 2 mL sterile containers (UniEquip GmbH). The PS concentration used was for thermal tests was 0.5 mM as it was pre-selected due to the high inactivation rates obtained under solar radiation (see results and discussion). Temperatures of  $30\pm 0.5$  °C,  $40\pm 0.5$  °C and  $50\pm 0.5$  °C were evaluated.

#### **2.4.2 Solar stirred tank reactors**

The bench scale solar experiments were performed in multiple 250 mL transparent vessels (DURAN-glass) magnetically stirred (150 rpm) covered with Duran glass lids. A range of PS concentrations, 0.01, 0.05, 0.1, 0.2, 0.5, 0.7 mM in IW and 0.2, 0.5, 0.7 and 1 mM in SUWW, were evaluated. The reactors were exposed to natural solar radiation for 3 hours.

#### **2.4.3 Solar Compound Parabolic Collector (CPC) reactor**

The pilot scale solar experiments were carried out in a re-circulated batch system, a Compound Parabolic Collector (CPC) reactor of 60 L (total volume) and 4.5 m<sup>2</sup> of CPC area exposed to the sun, as described elsewhere [38]. The recirculation flow rate was 30 L/min and the water temperature was controlled and maintained constant for the duration of the experiments using a heating-cooling system adapted to this reactor.

#### **2.5 Solar radiation measurements**

A solar UV pyranometer (CUV4, Kipp & Zonen) recorded every second the irradiance in the range 300-400 nm horizontally and at 37 ° (same inclination as the CPC module). The data was collected in terms of UV irradiance (Wm<sup>-2</sup>) (Figure S2). The horizontally collected data were used for the evaluation of solar energy dose received in the stirred vessel reactors, and the inclined (37°) UV radiation data were used for the CPC reactor, which is inclined at 37° over the horizontal.

#### **2.6 Disinfection kinetics**

The inactivation kinetics of *E. coli* and *E. faecalis* followed a typical two phase behaviour and were fitted to a simple model commonly used for disinfection with AOPs as reported

elsewhere [38-40]. In summary, the kinetics curve obeys to a first lag phase, also called ‘shoulder’, in which the concentration of viable bacteria remains stable, followed by a log-linear decay phase, which can be described by the classical Chick’ Law widely used in disinfection in a wide range of bacterial inactivation processes. Table 1 shows the analysis of the experimental data with the corresponding kinetic constants in the linear phase ( $k$ ,  $\text{min}^{-1}$ ) and shoulder length in the initial lag phase ( $SL$ , min).

### 3. RESULTS AND DISCUSSION

#### 3.1 Effect of temperature on inactivation of bacteria by PS in the dark – bench scale

The thermal effect of a range of temperatures reached during solar tests, 25, 30, 40 and 50 °C, was analysed in the presence (0.5 mM) and absence (control) of PS (Figure 1). The PS concentration and temperature values remained constant during 5 h of exposure (Figure S3). The present results show that *E. coli* thermal profiles at 30 °C, 40 °C and 50 °C obey the expected behaviour for this bacterium [14]. Similar behaviour was observed for *E. faecalis*. The thermal inactivation of both bacteria at temperatures between 25 and 30 °C is negligible, while it is significant at temperatures above 40 °C, being markedly fast at 50 °C.

The results in Figure 1 and the kinetic constants (Table 1) at 30 °C show that the presence of 0.5 mM-PS in the dark does not produce any significant bacterial decrease in both, *E. coli* and *E. faecalis*. At 40 °C the thermal effect over *E. coli* produced a 1.7-LRV in 5 h, while in the presence of 0.5 mM-PS a 3-LRV is observed in 4 h; and both described a first order kinetics without any lag phase (Table 1). On the other hand, *E. faecalis* shows a 3.5-LRV at 40 °C in 4 h, while the presence of 0.5 mM-PS at 40 °C leads to 5-LRV in 4h. Although the presence of PS makes the inactivation faster, both kinetics are very similar though and with an initial lag phase of 1 h. This clearly confirms that for

temperature rising from 30 to 40 °C the presence of PS has a marked effect on *E. coli* (Figure 1a) and less effect on *E. faecalis* (Figure 1b). The results at 50 °C revealed that the mere thermal effect of 50 °C has a dominant role, with a fast bacterial decay for both bacteria, which overlaps the effect of a possible thermal activation of PS at such temperature.

PS has been known to be thermally activated at temperatures between 40 and 70 °C [41]. For each mole of PS, two moles of sulfate radicals are generated, therefore increasing temperature might produce faster inactivation [42]. Nevertheless, the results in figure 1 cannot confirm the thermal PS activation as at temperatures above 50 °C bacteria easily die and the effect of PS is hardly differentiated. The concentration of PS measured during these experiments (Figure S3) showed stable values, suggesting that there is not significant dissociation of PS in any of the temperatures evaluated. Despite the PS stable concentration measured in all the experiments, for 40 °C the data revealed an increase in the inactivation rate in comparison with the experiment without PS, what may also suggest that PS is being dissociated.

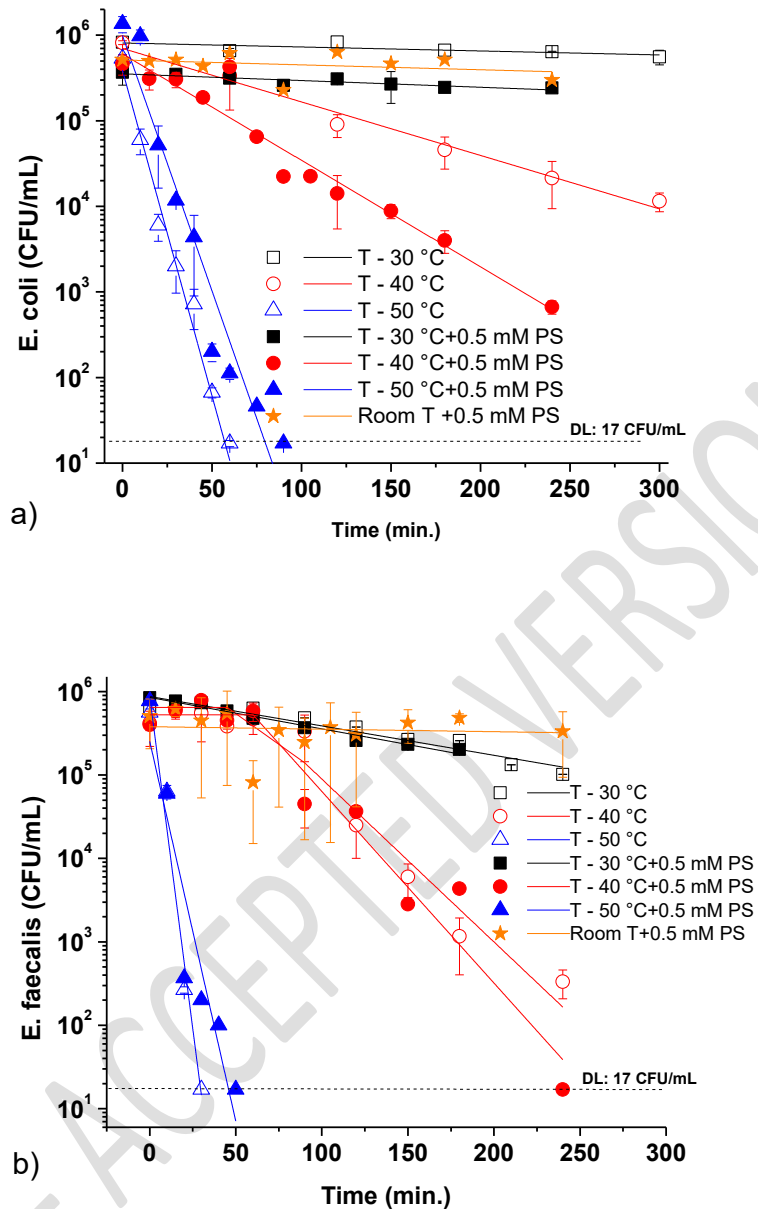


**Figure 1.** Influence of temperature on *E. coli* (a) and *E. faecalis* (b) inactivation and PS activation in the dark. 0.5 mM of PS, bench scale reactor.

### 3.2 Solar UVA PS activation – bench scale

The effect of different concentrations of PS (0.00, 0.01, 0.05, 0.1, 0.2, 0.5, 0.7 mM) on bacteria inactivation was investigated in IW (Figure 2).

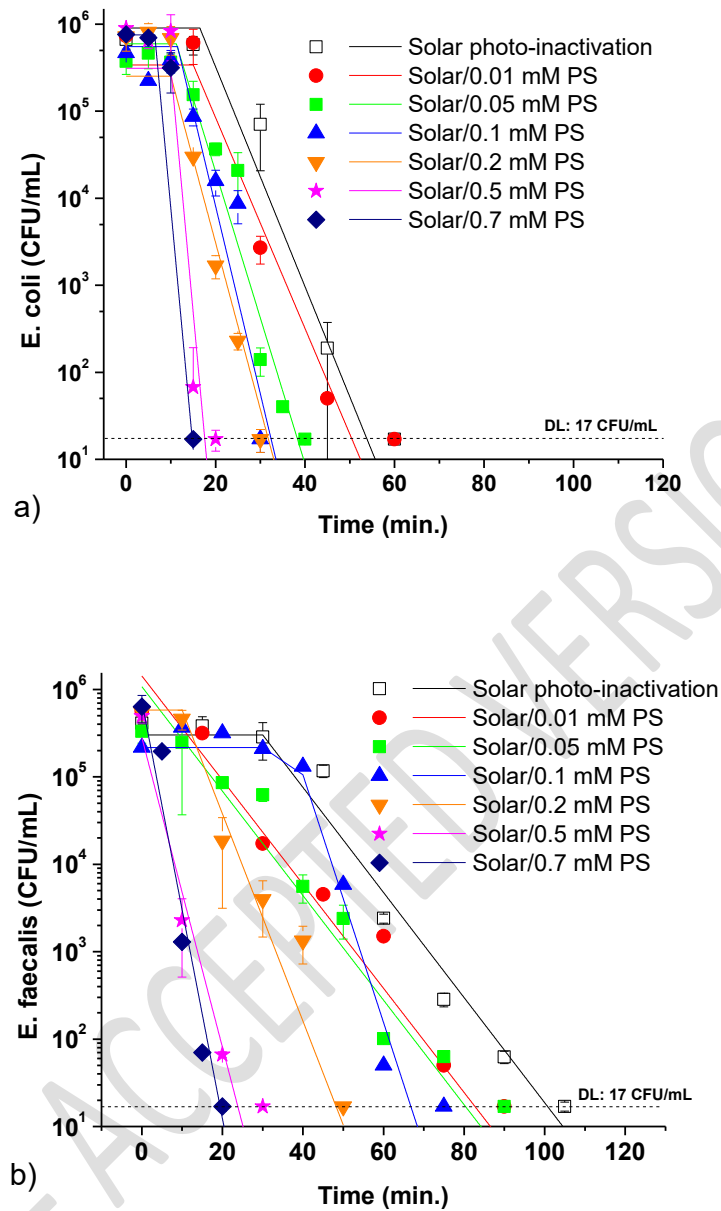


**Figure 2.** Inactivation of *E. coli* (a) and *E. faecalis* (b) in IW within several concentrations of PS under natural sunlight: 0.01, 0.05, 0.1, 0.2, 0.5, 0.7 mM and solar only disinfection, bench scale reactor ( $T_{0\text{min}} = 25 \pm 2 \text{ }^\circ\text{C}$  and  $T_{120\text{min}} = 35\text{-}45 \text{ }^\circ\text{C}$ ).

Solar UVA irradiance measured during solar tests ranged from  $26.38 \pm 1.27$  to  $44.44 \pm 1.4 \text{ Wm}^{-2}$ , corresponding to two hours of solar exposure from 10:00 AM to 12:00 PM local time. The temperature of the solar stirred tank reactors increased from  $25 \pm 2 \text{ }^\circ\text{C}$  at the beginning of the experiment to  $35\text{-}45 \text{ }^\circ\text{C}$  at the end after 2 h. The control

tests in the dark at the highest PS concentration (0.7 mM) did not reveal any loss in the viability of both pathogens (data not shown), therefore the inactivation of bacteria can be attributed to the combined effect of PS and solar radiation. The results of PS/solar UVA showed a gradual rate of bacterial inactivation, which becomes faster at increasing PS concentrations. The time required to achieve a 6-LRV of *E. coli* was 60 min, in the absence of PS, while only 15 min of solar exposure were required with 0.7 mM PS (Figure 2a). A similar behaviour of PS and solar illumination is observed for *E. faecalis* (Figure 2b), but it required longer exposure time periods (nearly double the times of *E. coli*) to reach a similar log-reduction. Clearly the presence of PS enhanced the bacterial inactivation as compared with the effect of solar radiation. Similar solar disinfection (without PS) results have been reported for both bacteria [5,43]. The bactericidal effect of sunlight is attributed to the cumulative oxidative action of UVA&B radiation internal and externally over bacteria [44]. The activation of PS under solar exposure is suggested to be due to the UV radiation adsorption via the O–O bond and the PS extinction coefficient, which is higher under the UV range, therefore it will enhance the activation rate by radiation [45]. The energy required to provoke the homolytic cleavage of PS is 140.2 kJ/mol, which is lower than other precursors of reactive oxygen species, such as H<sub>2</sub>O<sub>2</sub> (195.4 kJ/mol) [42,46]. Moreover, the concentration of PS measured during experiments showed stable values in all cases (see Figure S4). The PS dissociation cannot be confirmed by this methodology, however the results showed faster bacterial inactivation rates when increasing PS concentrations.

The kinetic analysis of the inactivation curves (Table 1) for *E. coli* clearly shows that the inactivation profiles obey to a log-linear decay after a short period of latency with ‘shoulder length’ values between 10 to 15 minutes. This shoulder is commonly observed in the disinfection kinetics of other disinfection processes [40], which is explained as the

time period required for the bacteria consortium to show the detrimental effects of the oxidative process.

**Table 1.** The kinetic model used in each case has been selected based on the higher root mean square obtained for different models.

[PS] (mM)	<i>E. coli</i>					<i>E. faecalis</i>				
	k (min <sup>-1</sup> )	R <sup>2</sup>	SL (min)	DL	Phase	k (min <sup>-1</sup> )	R <sup>2</sup>	SL (min)	DL	Phase
<b>Figure 1: Isotonic Water+ Dark + Temperature + PS</b>										
30 °C	NA*	-	-	N	2	NA*	-	-	N	2
40 °C	NA*	-	-	N	2	0.019±0.003	0.901	60	N	1
50 °C	0.076±0.004	0.984	-	Y	2	0.159±0.018	0.960	-	Y	2
30 °C+0.5	NA*	-	-	N	2	NA*	-	-	N	2
40 °C+0.5	0.012±0.001	0.937	-	N	2	0.023±0.003	0.914	60	Y	1
50 °C+0.5	0.060±0.004	0.960	-	Y	2	0.091±0.015	0.869	-	Y	2
T <sub>Free</sub> +0.5	NA*	-	-	N	2	NA*	-	-	N	2
<b>Figure 2: Isotonic Water + Solar radiation + PS</b>										
Solar only	0.126±0.015	0.971	15	Y	1	0.060±0.004	0.975	30	Y	1
0.01	0.121±0.010	0.979	15	Y	1	0.059±0.005	0.955	10	Y	2
0.05	0.168±0.015	0.949	10	Y	1	0.060±0.005	0.954	20	Y	2
0.1	0.215±0.033	0.892	10	Y	1	0.141±0.016	0.964	40	Y	1
0.2	0.191±0.017	0.955	10	Y	1	0.119±0.022	0.870	10	Y	1
0.5	0.562±0.148	0.870	10	Y	1	0.177±0.014	0.981	-	Y	2
0.7	0.554±0.280	0.592	5	Y	1	0.239±0.023	0.957	-	Y	2
<b>Figure 3: Isotonic Water + Solar radiation+ Temperature + PS</b>										
Solar only	0.026±0.002	0.917	-	Y	2	0.033±0.002	0.963	10	Y	1
30 °C + 0.5	0.101±0.006	0.981	10	Y	1	0.064±0.007	0.908	10	Y	1
50 °C + 0.5	0.445±0.037	0.986	10	Y	1	0.113±0.012	0.924	-	Y	2
T <sub>Free</sub> + 0.5	0.110±0.017	0.891	10	Y	1	0.070±0.010	0.873	10	Y	1
Dark + 0.5	0.157±0.042	0.863	60	Y	1	0.158±0.042	0.868	60	Y	1
<b>Figure 4: Synthetic Wastewater + Solar radiation + PS</b>										
Solar only	0.036±0.004	0.912	30	Y	1	0.048±0.026	0.914	180	N	1
0.2	0.073±0.011	0.856	20	Y	1	0.052±0.008	0.898	45	Y	1
0.5	0.084±0.011	0.897	-	Y	2	0.078±0.014	0.880	15	Y	1
0.7	0.091±0.012	0.899	-	Y	2	0.094±0.013	0.942	30	Y	1
1	0.110±0.011	0.945	-	Y	2	0.068±0.008	0.926	-	Y	2
<b>Figure 5: Synthetic Wastewater + dark + Temperature + PS</b>										
30 °C	NA*	-	-	N	2	NA*	-	-	N	2
40 °C	NA*	-	-	N	2	NA*	-	-	N	2
50 °C	0.044±0.004	0.935	-	N	2	0.038±0.002	0.981	30	N	1
30 °C + 0.5	NA*	-	-	N	2	NA*	-	-	N	2
40 °C + 0.5	NA*	-	-	N	2	NA*	-	-	N	2
50 °C + 0.5	0.054±0.009	0.862	-	Y	2	0.063±0.004	0.974	15	Y	1

Model 1: Shoulder length (SL) + Log-Linear; Model 2: Log-linear;  
T<sub>Free</sub>: Laboratory temperature (~25 °C). DL: Detection limit, Y:Yes, N: No.  
\* NA: no fitting, i.e. bacterial concentration was constant ( $\pm 0.004 \text{ min}^{-1}$ ).



The higher the PS concentration used the shorter time was required to attain a 6-LRV for both bacteria with different first order kinetics. In the case of *E. coli*, the kinetic rate constant values varied from  $0.121\pm 0.010 \text{ min}^{-1}$  to  $0.562\pm 0.148 \text{ min}^{-1}$  (maximum value for 0.5 mM of PS), although the shoulder length was between 5 and 15 min in all cases. For *E. faecalis* the effect of PS concentration has a maximum for 0.7 mM with longer SL values, between 10 and 40 minutes for all cases. A higher resistance of *E. faecalis* as compared to *E. coli* against other solar AOPs has been already reported [2,5,47]. This was attributed to their different cell wall composition and outer membrane osmotic permeability. *E. coli* has a higher structural complexity but under osmotic stress, the cell wall deteriorates faster, what will boost the permeability, being susceptible to oxidative processes [5]. The adding of sufficient amounts of PS produces a significant change in the inactivation profile, provoking a relevant increase in the inactivation constant, where  $k$  increases up to 3-4 fold as compared with the solar experiment without PS. Despite attaining distinct PS maximum values, in terms of inactivation time no great differences are noticed (Figure 2), therefore 0.5 mM was considered the optimal concentration of PS, as required the lower amount for fast bacterial inactivation. When observing the separated bacterial/damaging effects of solar radiation (only) and PS (in the dark at 30 °C), we can see that the kinetic constant of the inactivation processes (Table 1) are  $0.126\pm 0.015 \text{ min}^{-1}$  and  $0.000\pm 0.004 \text{ min}^{-1}$ , respectively. Revealing the incapacity of PS to effectively inactivate bacteria by itself. Meanwhile the process of solar radiation with 0.5 mM-PS has an inactivation kinetic constant value equal to  $0.562\pm 0.148 \text{ min}^{-1}$  for *E. coli* and  $0.239\pm 0.023 \text{ min}^{-1}$  for *E. faecalis* with 0.7 mM-PS. This evidences the solar radiation may be photoactivation PS with a subsequent accelerated inactivation of *E. coli* and *E. faecalis* in water. These results are in agreement with previous contributions of UVA-activated persulfate for water disinfection [26,48,49].

### **3.3 Solar UVA and thermal PS activation – pilot scale**

The dual activation of PS by solar radiation and solar thermal heating and the inactivation of *E. coli* and *E. faecalis* in IW was further investigated in the 60 L-CPC pilot scale reactor using 0.5 mM of PS. The thermal factor was considered under three tests, one exposed to the natural solar heating happening in the CPC reactor during the experiments, this is from 30 °C at the start, increasing up to 39 °C in 1 h, 43 °C in 2 h, and 46 °C in 3 h (end of the experiment), and two other at constant temperatures, 30 °C and 50 °C, achieved by a thermal control system installed in the reactor. Two additional control runs were performed: i) a solar photo-inactivation experiment to determine the effect of solar UV and solar heating effects on the bacterial survival; and ii) a dark control in the reactor with 0.5 mM PS under solar heating, to determine the thermal activation effect of PS under solar mild temperatures (50 °C).

Solar UVA radiation averaged among the entire solar tests performed at pilot scale ranged from  $23.29 \pm 12.27$  to  $44.60 \pm 1.21$   $\text{Wm}^{-2}$ , starting at 10:15 am local time and lasting 2.5 h of solar exposure.

The results show that dark thermal PS activation occurs after 1 hour (Figure 3), which explains the fast inactivation observed thereafter, obeying a first order kinetics. For both bacteria the inactivation profiles found followed similar trends.

The photo-thermal activation of PS at solar mild temperatures clearly shows inactivation results that fit in between the solar activated at 30 °C and 50 °C, which is to be expected given the thermal pattern observed in the CPC reactor. This highlights the concerted effect of solar UV and solar thermal heating in enhancing the water disinfection at pilot scale using PS. PS activation both through solar UVA and solar thermal in the CPC reactor contributed to enhance system efficiency, when compared to the solar UVA and solar

thermal separately, thus reducing inactivation time in about 30 minutes. Supposedly, when gathering the two activators, more peroxide bonds are disrupted and consequently the generation of sulfate radicals will be higher [45]. It is expected that the concerted effect would be a sum of both energies received by PS, translating into a more promptly inactivation.

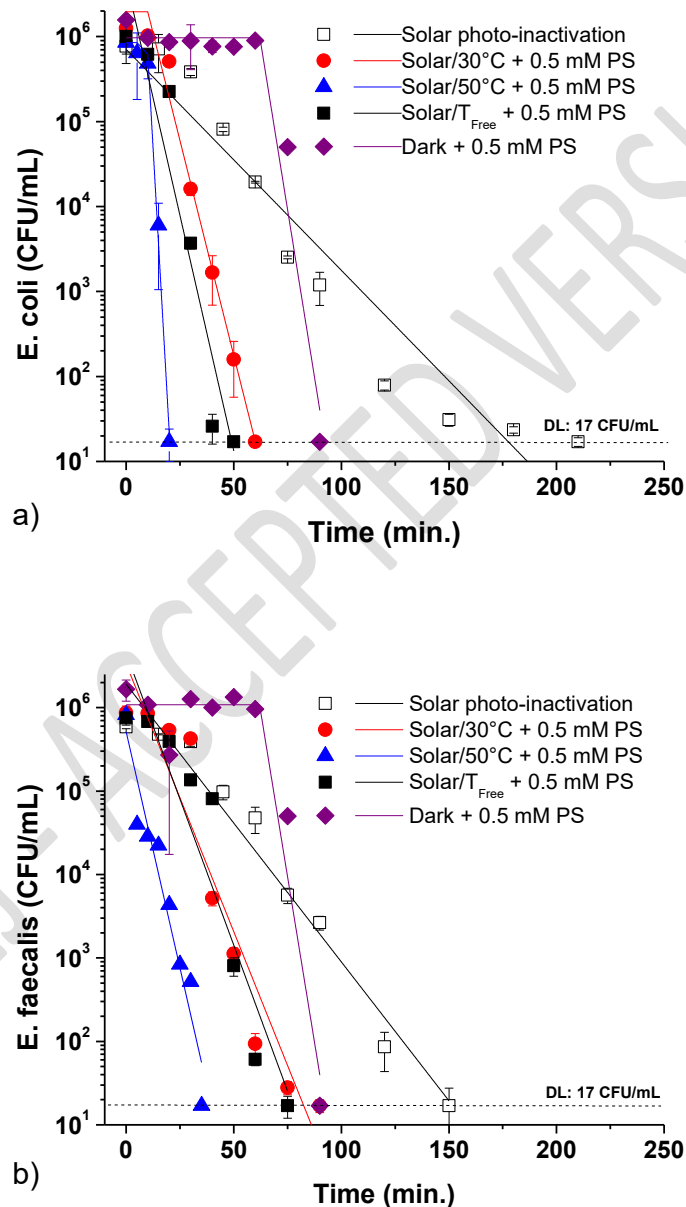


**Figure 3.** Influence of temperature and solar radiation on *E. coli* (a) and *E. faecalis* (b) inactivation with 0.5 mM of PS in a solar CPC reactor in IW, at pilot scale (60 L) ( $T_{Free}$ :  $T_{0min} = 30$  °C,  $T_{60min} = 39$  °C,  $T_{120min} = 43$  °C and  $T_{180min} = 46$  °C;  $T_{Dark} = 50$  °C).

The impact of temperature on other solar AOPs has been previously investigated. High temperatures have been reported to increase the intracellular pH, membrane potential and its permeability and also the generation of reactive oxygen species leading to cell injury [43,50]. Recently the synergistic effect of solar mild heat and solar UVA has been reported and mathematically modelled in solar reactors, under the well-known process SODIS (solar water disinfection) [51]. TiO<sub>2</sub> heterogeneous photocatalysis applied to water disinfection at pilot scale has also been reported to proceed at faster rates by increasing the water temperature (from 15 °C to 45 °C) for the inactivation of *E. coli* and *F. solani* [36]. Similarly the contribution of Ortega-Gómez et al. (2012) reported also beneficial effects of solar mild temperatures when using solar photo-Fenton for *E. faecalis* inactivation [52]. Marjanovic and collaborators (2018) reported an enhancement in the reaction inactivation rates when the solar and thermal effects were combined to activate PS. For PS solar activation, the quantum yield is less than 1 (25 °C). Moreover, adding the thermal effect, a lower amount of solar energy will be necessary to activate PS [25].

### **3.4 PS activation in SUWW– bench scale**

#### **3.4.1 Persulfate + sunlight**

The influence of organic matter during bacterial inactivation by solar and thermal activation of PS was also investigated. Figure 4 (a, b) shows the inactivation kinetics of *E. coli* and *E. faecalis* in SUWW under solar radiation with concentrations of PS ranged from 0.2 to 1 mM. As we observed for IW, the addition of PS accelerates the inactivation of both bacteria in comparison with solar disinfection alone. In this case, the concentration of PS that led to the highest inactivation kinetic rate (Table 1) was 1 mM for *E. coli* and 0.7 mM for *E. faecalis*, which is in agreement with the obtained data in IW (Figure 2) for

*E. faecalis*. Additionally, similar results regarding the observed kinetics shape and level of resistance of each bacterium were found. *E. coli* was more sensitive to the treatment than *E. faecalis*. Nevertheless, significant lower inactivation rate constants were obtained in SUWW compared to IW. Taking into consideration the highest inactivation rates for both in SUWW and IW, the  $k$  values were 5.1-fold lower for *E. coli* and 2.5-fold lower for *E. faecalis* in SUWW compared to IW (Table 1).

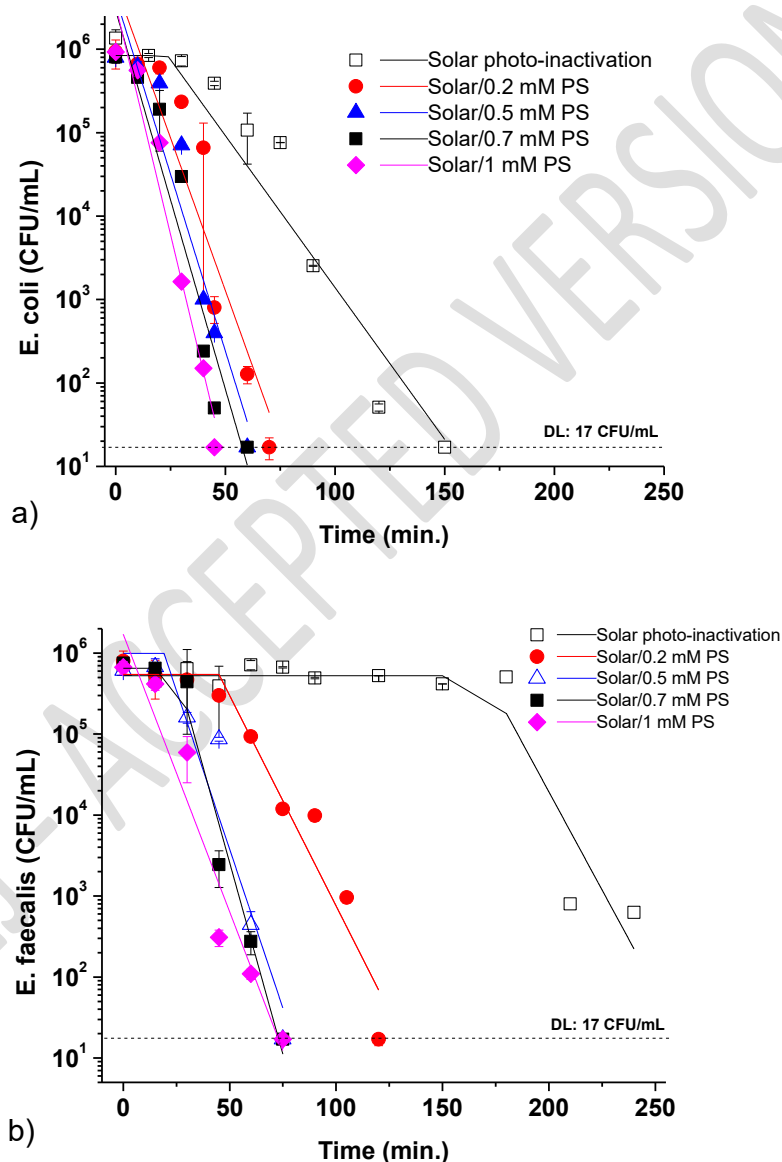


**Figure 4.** Inactivation of *E. coli* (a) and *E. faecalis* (b) in SUWW with several concentrations of PS under natural sunlight: 0.2, 0.5, 0.7 and 1 mM and solar only disinfection, at bench scale ( $T_{0min} = 25 \pm 2$  °C and  $T_{120min} = 35-45$  °C).

As aforementioned, PS is stable and can be activated in solution at several pH, but the  $\text{SO}_4^{\bullet-}$  generation rate is dependent on the pH value [31,53,54]. In this study the working pH of the SUWW was  $8.15 \pm 0.30$  and the measurements of dissolved organic carbon (DOC) during the process did not show significant degradation (data not shown). Additionally, the concentration of PS remained constant (Figure S2). The presence of DOC ( $25 \pm 5$  mg/L) turned the inactivation process harder. The possible reactions occurring between  $\text{SO}_4^{\bullet-}$  and DOC may be another reason for not achieving sufficiently high disinfection levels, once it seems that there are not being generated enough radicals at this pH, in comparison with the case of IW (at pH  $5.5 \pm 0.25$ ). In fact, the pH is an additional factor affecting the inactivation efficiency, once the generation of sulfate radicals is higher when the solution pH is lower than 7. Several authors analysed the formation rate of sulfate radicals and hydroxyl radicals under different pH and concluded that below pH 7  $\text{SO}_4^{\bullet-}$  are majorly formed, at pH = 9  $\text{SO}_4^{\bullet-}$  and hydroxyl radicals are being similarly generated and at pH > 9 the prevailing radicals are the hydroxyl radicals [31,54]. It is also known that the reaction of DOC with  $\text{SO}_4^{\bullet-}$  proceed at lower rates ( $6.8 \times 10^3$   $\text{mgC}^{-1}\text{s}^{-1}$ ) compared to the reaction with other radicals such as the hydroxyl radical ( $1.4 \times 10^4$   $\text{mgC}^{-1}\text{s}^{-1}$ ) [55], due to the hydrogen-abstraction reactions being slower in  $\text{SO}_4^{\bullet-}$  [53]. In addition,  $\text{SO}_4^{\bullet-}$  may react with several common anionic species present in water, including  $\text{HCO}_3^-$ ,  $\text{HPO}_4^{2-}$ ,  $\text{Cl}^-$  and  $\text{CO}_3^{2-}$  ending in weaker radicals [55], or even quench them [54], what may also help to explain the lower inactivation kinetics rates obtained in SUWW compared with IW. Furthermore, the scavenging effect of  $\text{Cl}^-$  can act in two ways: it can compromise UV PS activation, or can form chlorine or dichlorine radicals which are able to react more selectively [56], what can increase the efficiency in some cases. Therefore, in the presence of DOC = 25 mg/L, pH changes did not drive the sulfate radicals generation process via activation of PS.

### 3.4.2 Persulfate + temperature (dark)

The thermal activation of PS in the presence of organic matter was also investigated.

Figure 5 shows the inactivation of *E. coli* and *E. faecalis* at several temperatures in dark (30, 40 and 50 °C) with and without 0.5 mM of PS.

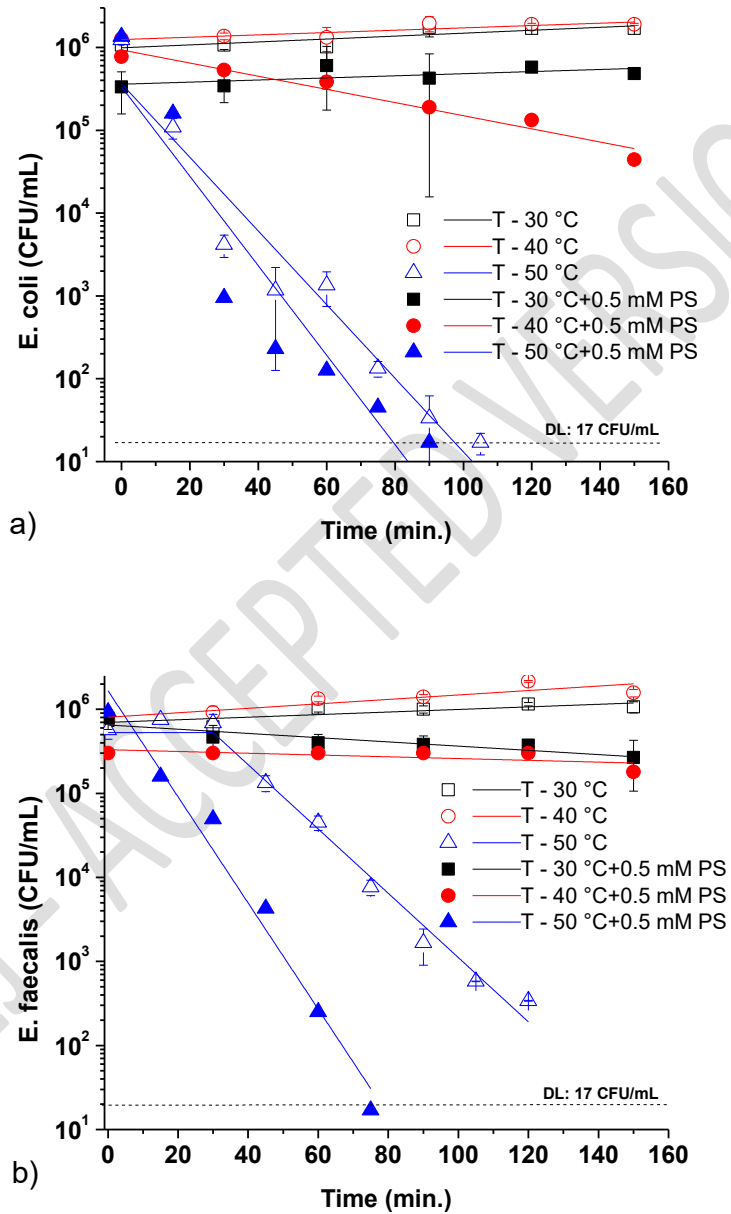


**Figure 5.** Influence of temperature on *E. coli* (a) and *E. faecalis* (b) inactivation and PS activation in the dark with 0.5 mM of PS in SUWW, at bench scale.

The inactivation trend obtained revealed that temperatures lower than 40 °C do not show any significant detrimental effect on bacterial viability, both with and without PS. Only at 50 °C the detection limit was reached within 80 min in presence of PS compared with the absence of PS (100 min), for both bacteria. This result is consistent with the results also found in IW (Figure 1); demonstrating the thermal activation of PS by mild-heat temperatures, in this case 50 °C. The higher energy was able to disrupt the peroxide bond, in order to generate the sulfate radicals. The prompt conversion of sulfate radicals into hydroxyl radicals, make these last radicals the major contributor for the process [54]. On the other hand, lower inactivation kinetics rates were again obtained in SUWW compared to IW due to the presence of DOC.

## CONCLUSIONS

In this study, the activation of persulfate by solar radiation and mild heat for water disinfection has been demonstrated in both IW and SUWW.

Regarding the thermal activation of PS, 50 °C leads to a more effective inactivation than at 40 °C with 0.5 mM of PS, highlighting the influence of temperature in the proper inactivation. *E. coli* revealed more thermal resistance than *E. faecalis*.

The efficiency of solar PS for the inactivation of *E. coli* and *E. faecalis* in IW generation has been proven. The highest inactivation rate constants for both bacteria were obtained for 0.5 and 0.7 mM of persulfate, requiring only 20 minutes of solar exposure to achieve the detection limit for *E. coli* and *E. faecalis*, respectively.

The scaling-up of the process using a pilot solar reactor of 60 L total treatment capacity has been successfully proven for 0.5 mM of PS with solar radiation.

Regarding the disinfection of SUWW, where the presence of organic matter becomes an added difficulty for disinfection, 1 and 0.7 mM of PS were found to be the best



concentrations for the inactivation of *E. coli* and *E. faecalis*, respectively via solar (optical and thermal) with PS, showing similar inactivation kinetics trend as in IW.

Finally, the proposed method demonstrates promising results for the disinfection of wastewater. 6-log reduction value levels have been achieved using low amounts of PS (0.5 mM) and solar radiation during periods of time below 2 hours. This solar treatment still needs more research in real urban wastewater samples at large scale. Additionally, it is necessary to find a methodology capable of measuring PS anions or sulfate radicals coming from the UVA solar and thermal activations. Nevertheless, the present work showed very promising results in terms of water disinfection.

#### **CONFLICTS OF INTEREST**

There are no conflicts to declare.

#### **ACKNOWLEDGEMENTS**

The authors acknowledge the financial support provided by SFERA - Solar Facilities for the European Research Area (228296) and by the FCT-Portuguese Foundation for Science and Technology (PD/BD/128270/2017), under the Doctoral Programme “Agricultural Production Chains – from fork to farm” (PD/00122/2012). Marco S. Lucas also acknowledges the funding provided by the European Union’s Horizon 2020 research and innovation programme under the Marie Skłodowska-Curie grant agreement No 660969.

#### **REFERENCES**

- [1] C. Han, J. Lalley, D. Namboodiri, K. Cromer, M.N. Nadagouda, Titanium dioxide-based antibacterial surfaces for water treatment, *Curr. Opin. Chem. Eng.* 11 (2016) 46-51. <https://doi.org/10.1016/j.coche.2015.11.007>.
- [2] A.Y. Booshehri, M.I. Polo-Lopez, M. Castro-Alferez, P. He, R. Xu, W. Rong, S. Malato, P. Fernández-Ibáñez, Assessment of solar photocatalysis using Ag/BiVO<sub>4</sub> at pilot solar Compound Parabolic Collector for inactivation of pathogens in well water and secondary effluents, *Catal. Today* 281 (2017) 124-134. <https://doi.org/10.1016/j.cattod.2016.08.016>.
- [3] K.L. Kotloff, J.P. Nataro, W.C. Blackwelder, D. Nasrin, T.H. Farag, S. Panchalingam, Y. Wu, S.O. Sow, D. Sur, R.F. Breiman, A.S.G. Faruque, A.K.M. Zaidi, D. Saha, P.L. Alonso, B. Tamboura, D. Sanogo, U. Onwuchekwa, B. Manna, T. Ramamurthy, S. Kanungo, J.B. Ochieng, R. Omere, J.O. Oundo, A. Hossain, S.K. Das, S. Ahmed, S. Qureshi, F. Quadri, R.A. Adegbola, M. Antonio, M.J. Hossain, A. Akinsola, I. Mandomando, T. Nhampossa, S. Acácio, K. Biswas, C.E. O'Reilly, E.D. Mintz, L.Y. Berkeley, K. Muhsen, H. Sommerfelt, R.M. Robins-Browne, M.M. Levine, Burden and aetiology of diarrhoeal disease in infants and young children in developing countries (the Global Enteric Multicenter Study, GEMS): a prospective, case-control study, *The Lancet*, 382 (2013) 209-222.
- [4] A. Flammini, M. Puri, L. Pluschke, O. Dubois, Walking the nexus talk: Assessing the Water-Energy-Food Nexus in the Context of the Sustainable Energy for All Initiative, Environment and Natural Resources Working Paper No. 58, FAO, Rome, 2014.
- [5] J. Rodríguez-Chueca, M.I. Polo-López, R. Mosteo, M.P. Ormad, P. Fernández-Ibáñez, Disinfection of real and simulated urban wastewater effluents using a mild solar photo-Fenton, *Appl. Catal. B: Environ.* 150–151 (2014) 619-629. <https://doi.org/10.1016/j.apcatb.2013.12.027>.

- [6] A. Bianco, M.I. Polo-López, P. Fernández-Ibáñez, M. Brigante, G. Mailhot, Disinfection of water inoculated with *Enterococcus faecalis* using solar/Fe(III)EDDS-H<sub>2</sub>O<sub>2</sub> or S<sub>2</sub>O<sub>8</sub><sup>2-</sup> process, *Water Res.* 118 (2017) 249-260. <https://doi.org/10.1016/j.watres.2017.03.061>.
- [7] S. Bounty, R.A. Rodriguez, K.G. Linden, Inactivation of adenovirus using low-dose UV/H<sub>2</sub>O<sub>2</sub> advanced oxidation, *Water Res.* 46 (2012) 6273-6278. <https://doi.org/10.1016/j.watres.2012.08.036>.
- [8] M. Cho, H. Chung, W. Choi, J. Yoon, Linear correlation between inactivation of *E. coli* and OH radical concentration in TiO<sub>2</sub> photocatalytic disinfection, *Water Res.* 38 (2004) 1069-1077. <https://doi.org/10.1016/j.watres.2003.10.029>.
- [9] M. Cho, J.-H. Kim, J. Yoon, Investigating synergism during sequential inactivation of *Bacillus subtilis* spores with several disinfectants, *Water Res.* 40 (2006) 2911-2920. <https://doi.org/10.1016/j.watres.2006.05.042>.
- [10] A. Ruiz-Aguirre, M.I. Polo-López, P. Fernández-Ibáñez, G. Zaragoza, Integration of Membrane Distillation with solar photo-Fenton for purification of water contaminated with *Bacillus* sp. and *Clostridium* sp. spores, *Sci. Total Environ.* 595 (2017) 110-118. <https://doi.org/10.1016/j.scitotenv.2017.03.238>.
- [11] W. Yu, Q. Wen, J. Yang, K. Xiao, Y. Zhu, S. Tao, Y. Lv, S. Liang, W. Fan, S. Zhu, B. Liu, H. Hou, J. Hu, Unraveling oxidation behaviors for intracellular and extracellular from different oxidants (HOCl vs. H<sub>2</sub>O<sub>2</sub>) catalyzed by ferrous iron in waste activated sludge dewatering. *Water Res.* 148 (2019) 60-69. <https://www.ncbi.nlm.nih.gov/pubmed/30347276>.
- [12] Y. Shi, J. Yang, W. Yu, S. Zhang, S. Liang, J. Song, Q. Xu, N. Ye, S. He, C. Yang, J. Hu, Synergetic conditioning of sewage sludge via Fe<sup>2+</sup>/persulfate and skeleton builder:

Effect on sludge characteristics and dewaterability, *Chem. Eng. J.* 270 (2015) 572-581.  
<https://www.sciencedirect.com/science/article/pii/S138589471500159X>.

[13] A. Fiorentino, G. Ferro, M.C. Alferez, M.I. Polo-López, P. Fernández-Ibañez, L. Rizzo, Inactivation and regrowth of multidrug resistant bacteria in urban wastewater after disinfection by solar-driven and chlorination processes, *J. Photochem. Photobiol. B: Biology* 148 (2015) 43–50. <https://doi.org/10.1016/j.jphotobiol.2015.03.029>.

[14] M. Castro-Alferez, M.I. Polo-López, J. Marugán, P. Fernández-Ibañez, Mechanistic modeling of UV and mild-heat synergistic effect on solar water disinfection, *Chem. Eng. J.* 316 (2017) 111-120. <https://doi.org/10.1016/j.cej.2017.01.026>.

[15] A.G. Gutierrez-Mata, S. Velazquez-Martínez, A. Álvarez-Gallegos, M. Ahmadi, J. A. Hernández-Pérez, F. Ghanbari, S. Silva-Martínez, Recent Overview of Solar Photocatalysis and Solar Photo-Fenton Processes for Wastewater Treatment – Review Article, *Int. J. Photoenergy* 8528063, (2017) 1-27. <https://doi.org/10.1155/2017/8528063>.

[16] P. Sun, C. Tyree, C.-H. Huang, Inactivation of *E. coli*, Bacteriophage MS2 and *Bacillus Spores* under UV/H<sub>2</sub>O<sub>2</sub> and UV/Peroxydisulfate Advanced Disinfection Conditions, *Environ. Sci. Technol.* 50 (2016) 4448-4458.  
<https://pubs.acs.org/doi/10.1021/acs.est.5b06097>.

[17] J. Rodríguez-Chueca, T. Silva, J.R. Fernandes, M.S. Lucas, G. Li Puma, J.A. Peres, A. Sampaio, Inactivation of pathogenic microorganisms in freshwater using HSO<sub>5</sub><sup>-</sup>/UV-A LED and HSO<sub>5</sub><sup>-</sup>/M<sup>n+</sup>/UV-A LED oxidation processes, *Water Res.* 123 (2017) 113-123.  
<https://doi.org/10.1016/j.watres.2017.06.021>.

[18] J. Moreno-Andrés, R. R. Quintero, A. Acevedo-Merino, E. Nebot, Disinfection performance using a UV/persulfate system: effects derived from different aqueous matrices, *Photochem. Photobiol. Sci.* 18 (2019) 878-883.  
<https://pubs.rsc.org/en/content/articlelanding/2019/pp/c8pp00304a>.

- [19] L. Chen, M. Tang, C. Chen, M. Chen, K. Luo, J. Xu, D. Zhou, F. Wu, Efficient Bacterial Inactivation by Transition Metal Catalyzed Auto-Oxidation of Sulfite, *Environ. Sci. Technol.* 51, 21 (2017) 12663-12671. <https://pubs.acs.org/doi/abs/10.1021/acs.est.7b03705>.
- [20] R.H. Waldemer, P.G. Tratnyek, R.L. Johnson, J.T. Nurmi, Oxidation of Chlorinated Ethenes by Heat-Activated Persulfate: Kinetics and Products, *Environ. Sci. Technol.* 41 (2007) 1010-1015. <https://pubs.acs.org/doi/abs/10.1021/es062237m>.
- [21] M. Ahmadi, J. Behin, A.R. Mahnam, Kinetics and thermodynamics of peroxydisulfate oxidation of Reactive Yellow 84, *J. Saudi Chem. Soc.* 20 (2016) 644-650. <https://doi.org/10.1016/j.jscs.2013.07.004>.
- [22] N. Garkusheva, G. Matafonova, I. Tsenter, S. Beck, V. Batoev, K. Linden, Simultaneous atrazine degradation and *E. coli* inactivation by simulated solar photo-Fenton-like process using persulfate, *J. Environ. Sci. Health, Part A* 52 (2017) 849-855. <https://doi.org/10.1080/10934529.2017.1312188>.
- [23] Y. Ji, L. Wang, M. Jiang, J. Lu, C. Ferronato, J.M. Chovelon, The role of nitrite in sulfate radical-based degradation of phenolic compounds: An unexpected nitration process relevant to groundwater remediation by *in-situ* chemical oxidation (ISCO), *Water Res.* 123 (2017) 249-257. <https://doi.org/10.1016/j.watres.2017.06.081>.
- [24] L. Lian, B. Yao, S. Hou, J. Fang, S. Yan, W. Song, Kinetic Study of Hydroxyl and Sulfate Radical-Mediated Oxidation of Pharmaceuticals in Wastewater effluents, *Environ. Sci. Technol.* 51 (2017) 2954-2962. <https://pubs.acs.org/doi/abs/10.1021/acs.est.6b05536>.
- [25] M. Marjanovic, S. Giannakis, D. Grandjean, L.F. de Alencastro, C. Pulgarin, Effect of  $\mu\text{M}$  Fe addition, mild heat and solar UV on sulfate radical-mediated inactivation of

bacteria, viruses, and micropollutant degradation in water, *Water Res.* 140 (2018) 220-231. <https://doi.org/10.1016/j.watres.2018.04.054>.

[26] M.G. Antoniou, A.A. de la Cruz, D.D. Dionysiou, Degradation of microcystin-LR using sulfate radicals generated through photolysis, thermolysis and  $e^-$  transfer mechanisms, *Appl. Catal. B: Environ.* 96 (2010) 290-298. <https://doi.org/10.1016/j.apcatb.2010.02.013>.

[27] C. Liang, Z.-S. Wang, N. Mohanty, Influences of carbonate and chloride ions on persulfate oxidation of trichloroethylene at 20 °C, *Sci. Total Environ.* 370 (2006) 271-277. <https://doi.org/10.1016/j.scitotenv.2006.08.028>.

[28] Y.-F. Huang, Y.-H. Huang, Identification of produced powerful radicals involved in the mineralization of bisphenol A using a novel UV- $\text{Na}_2\text{S}_2\text{O}_8/\text{H}_2\text{O}_2\text{-Fe}$  (II, III) two-stage oxidation process, *J. Hazard. Mat.* 162 (2009) 1211-1216. <https://doi.org/10.1016/j.jhazmat.2008.06.008>.

[29] N. Potakis, Z. Frontistis, M. Antonopoulou, I. Konstantinou, D. Mantzavinos, Oxidation of bisphenol A in water by heat-activated persulfate, *J. Environ. Manag.* 195(2) (2017) 125-132. <https://doi.org/10.1016/j.jenvman.2016.05.045>.

[30] Y.-T. Lin, C. Liang, J.-H. Chen, Feasibility study of ultraviolet activated persulfate oxidation of phenol, *Chemosphere* 82 (2011) 1168-1172. <https://doi.org/10.1016/j.chemosphere.2010.12.027>.

[31] R. Hazime, Q.H.Nguyen, C. Ferronato, A. Salvador, F. Jaber, J.-M. Chovelon, Comparative study of imazalil degradation in three systems: UV/ $\text{TiO}_2$ , UV/ $\text{K}_2\text{S}_2\text{O}_8$  and UV/ $\text{TiO}_2/\text{K}_2\text{S}_2\text{O}_8$ , *Appl. Catal. B: Environ.* 144 (2014) 286-291. <https://doi.org/10.1016/j.apcatb.2013.07.001>.

- [32] H. Hermann, On the photolysis of simple anions and neutral molecules as sources of O<sup>-</sup>/OH, SO<sub>x</sub><sup>-</sup> and Cl in aqueous solution, *Phys. Chem. Chem. Phys.* 9 (2007) 3925-4032. 10.1039/B618565G.
- [33] I. Michael-Kordatou, M. Iacovou, Z. Frontistis, E. Hapeshi, D.D. Dionysiou, D. Fatta-Kassinos, Erythromycin oxidation and ERY-resistant *Escherichia coli* inactivation in urban wastewater by sulfate radical-based oxidation process under UV-C irradiation, *Water Res.* 85 (2015) 346-358. <https://doi.org/10.1016/j.watres.2015.08.050>.
- [34] D. Xia, H. He, H. Liu, Y. Wang, Q. Zhang, Y. Li, A. Lu, C. He, P.K. Wong, Persulfate-mediated catalytic and photocatalytic bacterial inactivation by magnetic natural ilmenite, *Appl. Catal. B: Environ.* 238 (2018) 70-81. <https://doi.org/10.1016/j.apcatb.2018.07.003>.
- [35] R. Xiao, K. Liu, L. Bai, D. Minakata, Y. Seo, R.K. Göktaş, D.D. Dionysiou, C.-J. Tang, Z. Wei, R. Spinney, Inactivation of pathogenic microorganisms by sulfate radical: Present and future - Review, *Chem. Eng. J.* 371 (2019) 222-232. <https://doi.org/10.1016/j.cej.2019.03.296>.
- [36] C. Liang, C-F. Huang, N. Mohanty, R.M. Kurakalva, A rapid spectrophotometric determination of persulfate anion in ISCO, *Chemosphere* 73 (2008) 1540-1543. <https://doi.org/10.1016/j.chemosphere.2008.08.043>.
- [37] M.I. Polo-López, I. García-Fernández, I. Oller, P. Fernández-Ibáñez, Solar disinfection of fungal spores in water aided by low concentrations of hydrogen peroxide, **Photochem. Photobiol. Sci.** 10 (2011) 381-388. <https://www.ncbi.nlm.nih.gov/pubmed/20859602>.
- [38] I. García-Fernández, I. Fernández-Calderero, M.I. Polo-López, P. Fernández-Ibáñez, Disinfection of urban effluents using solar TiO<sub>2</sub> photocatalysis: A study of significance of dissolved oxygen, temperature, type of microorganism and water matrix, *Catal. Today* 240 (2015) 30-38. <https://doi.org/10.1016/j.cattod.2014.03.026>.

- [39] G. Ferro, A. Fiorentino, M.C. Alferez, M.I. Polo-López, L. Rizzo, P. Fernández-Ibáñez, Urban wastewater disinfection for agricultural reuse: effect of solar driven AOPs in the inactivation of a multidrug resistant *E. coli* strain, *Appl. Catal. B: Environ.* 178 (2015) 65–73. <https://doi.org/10.1016/j.apcatb.2014.10.043>.
- [40] M.I. Polo-López, I. García-Fernández, T. Velegraki, A. Katsoni, I. Oller, D. Mantzavinos, P. Fernández-Ibáñez, Mild solar photo-Fenton: An effective tool for the removal of *Fusarium* from simulated municipal effluents, *Appl. Catal. B: Environ.* 111–112 (2012) 545–554. <https://doi.org/10.1016/j.apcatb.2011.11.006>.
- [41] G.P. Anipsitakis, D.D. Dionysiou, Degradation of Organic Contaminants in Water with Sulfate Radicals Generated by the Conjunction of Peroxymonosulfate with Cobalt, *Environ. Sci. Technol.* 37 (2003) 4790-4797. <https://pubs.acs.org/doi/abs/10.1021/es0263792>.
- [42] I.A. Ike, K. Linden, J. Orbell, M. Duke, Critical review of the science and sustainability of persulfate advanced oxidation processes, *Chem. Eng. J.* 338 (2018) 651-669. <https://doi.org/10.1016/j.cej.2018.01.034>.
- [43] M. Castro-Alferez, M.I. Polo-López, J. Marugán, P. Fernández-Ibáñez, Mechanistic model of the *Escherichia coli* inactivation by solar disinfection based on the photo-generation of internal ROS and the photo-inactivation of enzymes: CAT and SOD, *Chem. Eng. J.* 318 (2017) 214-223. <https://doi.org/10.1016/j.cej.2016.06.093>.
- [44] M. Castro-Alferez, M.I. Polo-López, P. Fernández-Ibáñez, Intracellular mechanisms of solar water disinfection, *Sci. Rep.* 6 (2016) 38145. <https://doi.org/10.1038/srep38145>.
- [45] M. Khandarkhaeva, A. Batoeva, D. Aseev, M. Sizykh, O. Tsydenova, Oxidation of atrazine in aqueous media by solar-enhanced Fenton-like process involving persulfate and ferrous ion, *Ecotoxicol. Environ. Saf.* 137 (2017) 35-41. <https://doi.org/10.1016/j.ecoenv.2016.11.013>.



- [46] S. Waclawek, H.V. Lutze, K. Grübel, V.V.T. Padil, M. Černík, D.D. Dionysiou, Chemistry of persulfates in water and wastewater treatment: A review, *Chem. Eng. J.* 330 (2017) 44-62. <https://doi.org/10.1016/j.cej.2017.07.132>.
- [47] R. van Grieken, J. Marugán, C. Pablos, L. Furones, A. López, Comparison between the photocatalytic inactivation of Gram-positive *E. faecalis* and Gram-negative *E. coli* faecal contamination indicator microorganisms, *Appl. Catal. B: Environ.* 100 (2010) 212-220. <https://doi.org/10.1016/j.apcatb.2010.07.034>.
- [48] J.A. Khan, X. He, N.S. Shah, H.M. Khan, E. Hapeshi, D. Fatta-Kassinos, D.D. Dionysiou, Kinetic and Mechanism Investigation on the Photochemical Degradation of Atrazine with Activated  $\text{H}_2\text{O}_2$ ,  $\text{S}_2\text{O}_8^{2-}$  and  $\text{HSO}_5^-$ , *Chem. Eng. J.* 252 (2014) 393-403. <https://doi.org/10.1016/j.cej.2014.04.104>.
- [49] J. Rodríguez-Chueca, C. Amor, T. Silva, D.D. Dionysiou, G. Li Puma, M.S. Lucas, J.A. Peres, Treatment of winery wastewater by sulphate radicals:  $\text{HSO}_5^-$ /transition metal/UV-A LEDs, *Chem. Eng. J.* 310 (2017) 473-483. <https://doi.org/10.1016/j.cej.2016.04.135>.
- [50] S. Baatout, P. de Boever, M. Mergeay, Temperature-induced changes in bacterial physiology as determined by flow cytometry, *Ann. Microbiol.* 55 (2005) 73–80.
- [51] M. Castro-Alfárez, M.I. Polo-López, J. Marugán, P. Fernández-Ibáñez, Validation of a solar-thermal water disinfection model for *Escherichia coli* inactivation in pilot scale solar reactors and real conditions, *Chem. Eng. J.* 331 (2018) 831-840. <https://doi.org/10.1016/j.cej.2017.09.015>.
- [52] E. Ortega-Gómez, P. Fernández-Ibáñez, M.M.B. Martín, M.I. Polo-López, B.E. García, J.A.S. Pérez, Water disinfection using photo-Fenton: Effect of temperature on *Enterococcus faecalis* survival, *Water Res.* 46 (2012) 6154-6162. <https://doi.org/10.1016/j.watres.2012.09.007>.

- [53] N.K.V. Leitner, Sulfate radical ion – based AOPs in: M.I. Stefan, Advanced Oxidation Processes for Water Treatment: Fundamentals and Applications, IWA Publishing, London, 2018, pp. 429-455.
- [54] J. Wang, S. Wang, Activation of persulfate (PS) and peroxymonosulfate (PMS) and application for the degradation of emerging contaminants - Review, Chem. Eng. J. 334 (2018) 1502-1517. <https://doi.org/10.1016/j.cej.2017.11.059>.
- [55] W.-D. Oh, Z. Dong, T.-T. Lim, Generation of sulfate radical through heterogeneous catalysis for organic contaminants removal: Current development, challenges and prospects, Appl. Catal. B: Environ. 194 (2016) 169-201. <https://doi.org/10.1016/j.apcatb.2016.04.003>.
- [56] W. Huang, A. Bianco, M. Brigante, G. Mailhot, UVA-UVB activation of hydrogen peroxide and persulfate for Advanced Oxidation Processes: Efficiency, mechanism and effect of various water constituents, J. Hazard. Mater. 347 (2018) 279-287. <https://doi.org/10.1016/j.jhazmat.2018.01.006>.

# Inactivation of water pathogens with solar photo-activated persulfate oxidation

L. C. Ferreira<sup>a</sup>, M. Castro-Alfárez<sup>b</sup>, S. Nahim-Granados<sup>b</sup>, M.I. Polo-López<sup>b</sup>, M. S. Lucas<sup>a,c\*</sup>, G. Li Puma<sup>c</sup>, P. Fernández-Ibáñez<sup>b,d</sup>

<sup>a</sup> Centro de Química de Vila Real, Universidade de Trás-os-Montes e Alto Douro, 5000-801 Vila Real, Portugal

<sup>b</sup> Plataforma Solar de Almería – CIEMAT, P.O. Box 22, 04200 Tabernas, Almería, Spain

<sup>c</sup> Environmental Nanocatalysis & Photoreaction Engineering, Department of Chemical Engineering, Loughborough University, Loughborough, LE11 3TU, United Kingdom

<sup>d</sup> Nanotechnology and Integrated BioEngineering Centre, School of Engineering, University of Ulster, Newtownabbey, Northern Ireland BT37 0QB, United Kingdom

Supplementary Material

\*Corresponding authors:

Marco S. Lucas; [mlucas@utad.pt](mailto:mlucas@utad.pt)

Pilar Fernández-Ibáñez; [p.fernandez@ulster.ac.uk](mailto:p.fernandez@ulster.ac.uk)

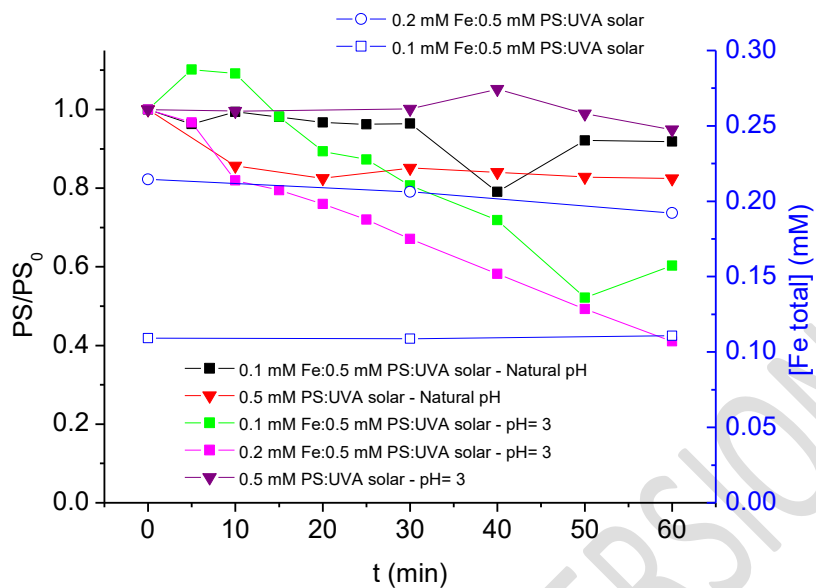


**Figure S1** – Persulfate anion concentration ( $[PS_0] = 0.5 \text{ mM}$ ) vs time and Total iron ( $[FeSO_4]_0 = 0.1$  and  $0.2 \text{ mM}$ ) vs time in natural pH and pH= 3. Spectrophotometric method adapted by Liang et al. 2008.

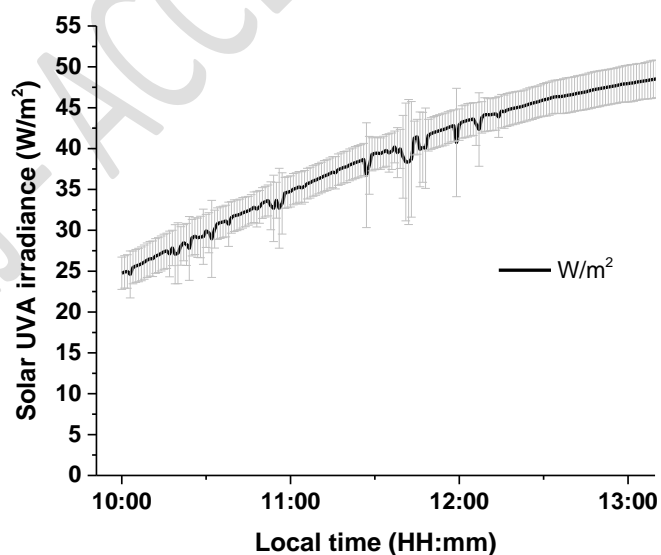


**Figure S2** - Average values of solar irradiance measured during the experiments.

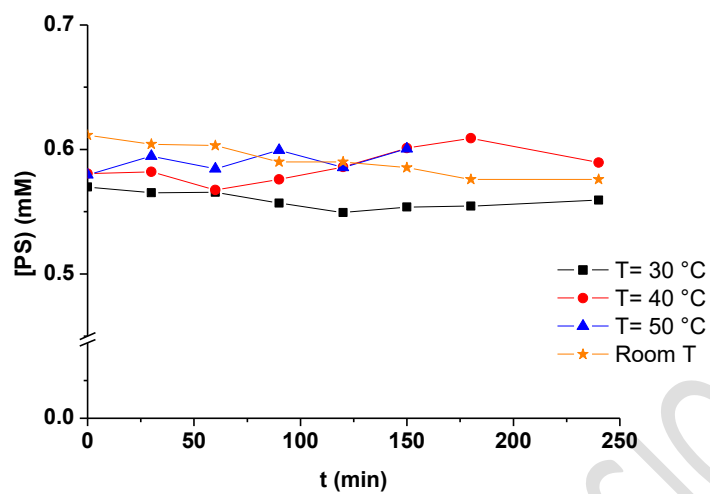


**Figure S3** - PS concentration during the experiments in the dark at 30 °C, 40 °C and 50 °C with 0.5 mM of PS.

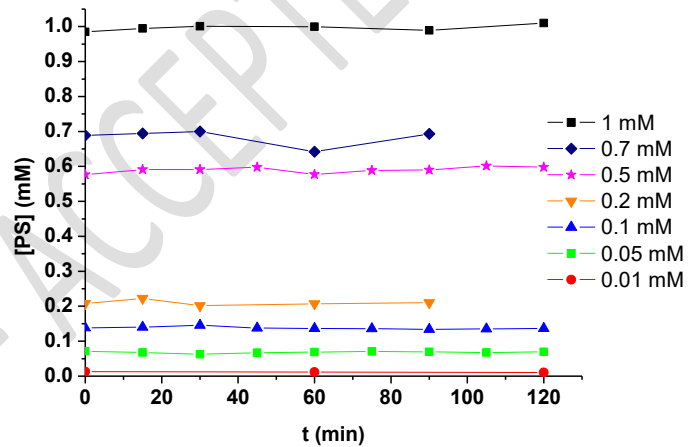


**Figure S4** - PS concentration during the experiments with IW and SUWW, at different temperatures.